Optik 139 (2017) 9–15

Contents lists available at ScienceDirect

Optik

journal homepage: www.elsevier.de/ijleo

Original research article

Electronic and optical properties of paratellurite TeO_2 under pressure: A first-principles calculation

Mosayeb Naseri[a], Jaafar Jalilian[b,*], A.H. Reshak[c,d]

[a] Department of Physics, Kermanshah Branch, Islamic Azad University, Kermanshah, Iran
[b] Young Researchers and Elite Club, Kermanshah Branch, Islamic Azad University, P.O. Box 6718997551, Kermanshah, Iran
[c] New Technologies – Research Centre, University of West Bohemia, Univerzitni 8, 306 14 Pilsen, Czech Republic
[d] School of Material Engineering, University Malaysia Perlis, 01007 Kangar, Perlis, Malaysia

ARTICLE INFO

Article history:
Received 29 December 2016
Accepted 24 March 2017

Keywords:
Density functional theory
α-TeO_2 crystal
Electronic properties
Optical properties

ABSTRACT

In this communication, the electronic and optical properties of paratellurite TeO_2 (α-TeO_2) single crystal under pressure up to 9 GPa are investigated by means of the first principles calculations in the framework of the density functional theory. The calculation show that by imposing external hydrostatic pressure, α-TeO_2 remains an indirect band gap semiconductor. However, by increasing the pressure from 0 to 9 GPa, the energy band gap of the α-TeO_2 crystal is increased. The calculated optical properties indicate a little blue shift in the optical properties spectra of the material.

1. Introduction

To predict pressure-dependent physical properties of materials from first principles studies alone has marked a fundamental step forward in investigating realistic materials properties. Due to the potential optical application of TeO_2 based glass such as optical switching devices, optical amplifiers, it has attracted considerable studies from theoretical and experimental point of view [1].

There are three crystalline phases of TeO_2. These are paratellurite α-TeO_2 (D_4^4, $P4_12_12$) [2,3], the tellurite β-TeO_2(D_{2h}^{15}, *Pbca*) [4–6], and γ-TeO_2. The first two phases have been known for long time, while the third crystalline polymorph which is metastable at normal conditions has been recently identified [7]. The TeO_2 phases are described as different arrangements of corner-sharing TeO_4 units including two longer Te–O bonds and two shorter ones [8]. The α-TeO_2 is thermodynamically stable, but naturally the TeO_2 is mostly found in β phase [9].

It has been reported that TeO_2 possesses the dielectric constant of about 17–28 in both TeO_2 crystal and films which proposes potential application of the compound in ultrahigh integration electronic devices, makes this compounds more attracting material [4,10–13]. Very recently the phase transition and equation of state of α-TeO_2 under high pressure have been studied by Liu et al. [14]. It has been shown that for paratellurite, in the condition of external pressure below 22 GPa, in which a first-order phase transition observed, the density increases continuously with pressure, whereas the lattice parameters a and c decrease with pressure, while b decreases slightly and begins to increase at about 10 GPa. The phenomena are considered as a precursor of the coming phase transition.

* Corresponding author.
E-mail address: jaafarjalilian@gmail.com (J. Jalilian).

http://dx.doi.org/10.1016/j.ijleo.2017.03.108
0030-4026/

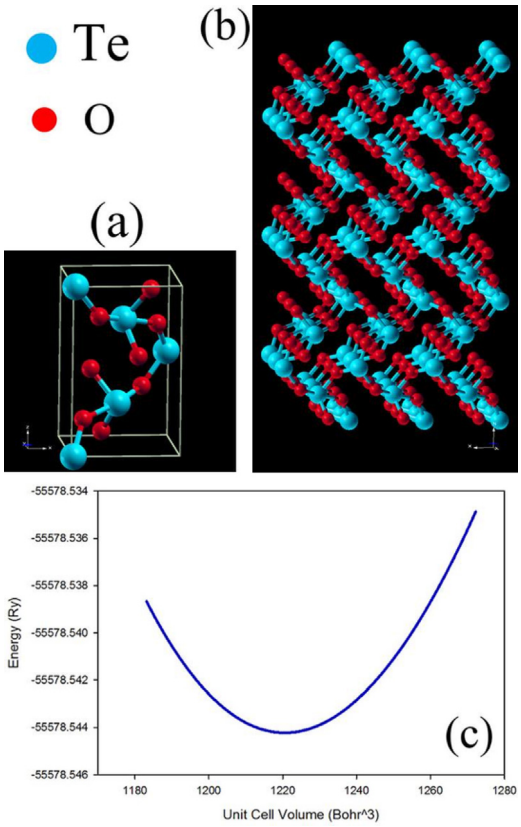

Fig. 1. (a) α-TeO_2 unit cell. (b) A supercell of α-TeO_2 crystal. (c) Energy vs volume of a α-TeO_2 unit cell.

In this study, the electronic and optical properties of the paratellurite TeO_2 under pressure up to 9 GPa have been studied using density functional theory.

2. Computational details

In this calculation, the density functional theory as implemented by the WIEN2k code [15] is used. To expand the Kohn–Sham wave functions, the all-electron full-potential linear augmented plane waves plus local orbital (FPLAPW + lo) is applied. The exchange-correlation term is produced by utilizing the generalized gradient approximation presented by Perdew–Burke–Ernzerhof (GGA-PBE) [16]. Based on Monkhorst–Pack approximation [17], a mesh of $11 \times 11 \times 7$ and $25 \times 25 \times 15$ have been considered in the whole first Brillouin zone for electronic and optical calculations, respectively. The computational input parameters are $R_{MT}K_{max} = 8$, G_{max}=14 $Ry^{1/2}$ and $l_{max} = 10$. To gain the complex dielectric function components, the random phase approximation (RPA) method [18] and the Kramers–Kronig relations are employed.

3. Structural properties

Prior to the calculation, the lattice constants of the α-TeO_2 (see Fig. 1a and b) is optimized using the thermodynamical equation state of Brich–Murnaghun [19]:

$$E(V) = E_0 + \frac{9B_0V_0}{16}\left\{\left[\left(\frac{V_0}{V}\right)^{2/3} - 1\right]^3 B_0'\right\} + \frac{9B_0V_0}{16}\left\{\left[\left(\frac{V_0}{V}\right)^{2/3} - 1\right]^2 \left[6 - 4\left(\frac{V_0}{V}\right)^{2/3}\right]\right\} \quad (1)$$

where V_0 is the initial considered volume, V is the deformed volume, B_0 is the bulk modulus, and B_0' is the derivative of the bulk modulus with respect to pressure. The energy vs volume curve for a unit cell of α-TeO_2 is plotted in Fig. 1c. The minimum of this plot provides the equilibrium volume of the crystal cell. Considering the obtained equilibrium volume, the optimized lattice constants are calculated as $a = b = 4.85$ Å and $c = 7.68$ Å which are in good agreement with the previous obtained values. The calculated optimized lattice parameters are compared with the previous obtained values in Table 1.

Table 1
Structural data for α-TeO_2. Both SIESTA and this work have used PBE-GGA approximation. The ESPRESSO and B3LYP have employed plane wave and hybrid functional calculation respectively.

	Experiment [21]	SIESTA [22]	ESPRESSO [23]	B3LYP [24]	This work
a(Å)	4.808	4.987	4.990	4.899	4.85
c(Å)	7.612	7.612	7.546	7.792	7.68
$(Te–O)_1$ (Å)	1.879	1.955	1.944	1.909	1.94
$(Te–O)_2$ (Å)	2.121	2.118	2.160	2.160	2.15

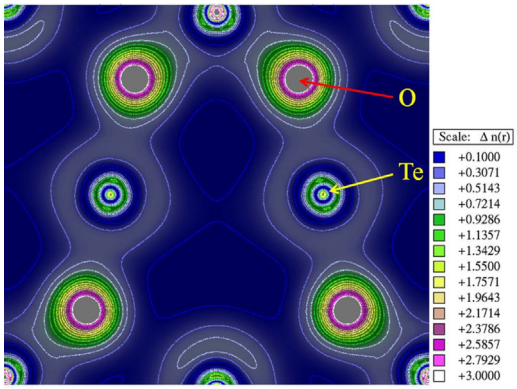

Fig. 2. A two-dimensional charge distribution in (110) plane, the red and blue balls illustrate oxygen and tellurium atoms respectively. (For interpretation of the references to color in this legend, the reader is referred to the web version of the article.)

The considered unit cell contains eight oxygen atoms and four tellurium atoms. Each tellurium atom is shared by four oxygen atoms while each oxygen atom is bounded by two tellurium atoms. After the energy optimization process, it has been found that the TeO_2 exhibits two different Te–O bond lengths, these are 1.94 and 2.15 Å.

The structural stability of the cell, is confirmed by cohesive energy calculation. According to the definition of cohesive energy:

$$E_{coh} = \frac{E^{total}_{\alpha-TeO_2} - mE^{isolated}_{Te} - nE^{isolated}_{O}}{m+n} \quad (2)$$

where $E^{total}_{\alpha-TeO_2}$, $E^{isolated}_{Te}$ and $E^{isolated}_{O}$ are total energy of α-TeO_2 unit cell, the energy of isolated tellurium and isolated oxygen atoms, respectively. Also, m and n indexes refer to the number of tellurium and oxygen atoms in the cell, respectively. We obtained the value of 3.21 eV/atom for cohesive energy of this compound which denotes to its a good structural stability.

4. Electronic properties

The electronic properties of the α-TeO_2 crystal under hydrostatic pressure up to 9 GPa were investigated. To understand the bond nature of Te–O in α-TeO_2 crystal, the two-dimensional charge distribution in (110) plane is plotted in Fig. 2. As can be seen from this figure, the charge accumulation around oxygen atom is more remarkable than tellurium atom, which is in agreement with the higher electron negativity of the oxygen atoms. Furthermore, by consideration on the electronic charge distribution plot, one can claim the covalence nature for the Te–O bonds.

To gain deep insight into the electronic properties of α-TeO_2, the total, partial density of states (DOS) and the band structure of the α-TeO_2 under different pressures are plotted in Figs. 3–5 respectively.

Considering the DOS plots (Fig. 3), one can see that for the considered structure the oxygen atoms play more considerable role in valance bands of the α-TeO_2 than the tellurium atoms, which is attributed to the higher electron negativity of oxygen than the tellurium, i.e., the bonding wave functions are concentrated around oxygen atoms. By comparing the total and partial density of states (DOS) plots at different pressures, one can see that imposing hydrostatic pressure up to 9 GPa to the considered crystal does not make considerable change in the valance bands structure. However, it is clear that by increasing hydrostatic pressure, the conduction bands edge is shifted to higher energies, i.e., a small blue shift is occurred in valance bands structure. On the other word, imposing hydrostatic pressure to the α-TeO_2, makes the Te–O bonds more stronger than that of pressure free α-TeO_2 crystal.

According to the band structure plots (Fig. 5), the considered compound exhibits an indirect energy gap of 2.85 eV, in which the valance bands maximum is occurred in somewhere between Γ and X directions, while the conduction bands minimum is located between Γ and M directions. The calculation shows that the energy gap of the α-TeO_2 is slightly increased under pressure, i.e., the material indicates band gaps of about 2.94 eV, 3.01 eV, and 3.07 eV under 3, 6, and 9 GPa pressure respectively.

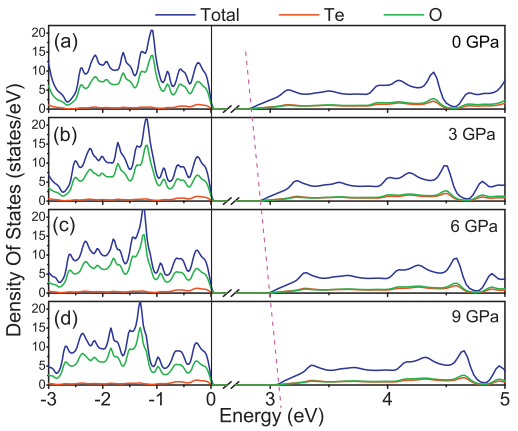

Fig. 3. The total and partial density of states (DOS) at different pressures. The blue, red, and green lines refer to total DOS, the total DOS of tellurium, and the total DOS of oxygen atoms. (For interpretation of the references to color in this legend, the reader is referred to the web version of the article.)

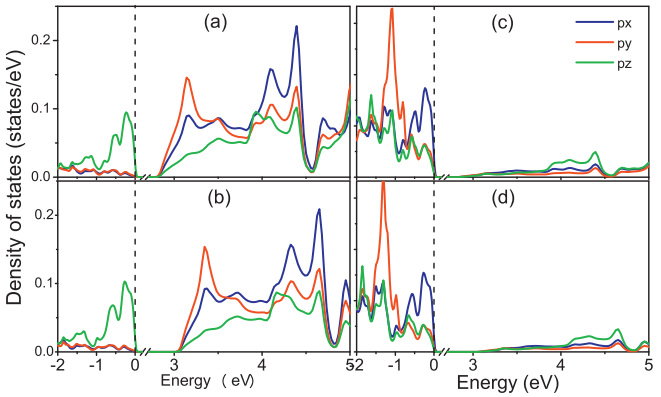

Fig. 4. The partial density of states (DOS) at different pressures. The blue, red, and green lines refer to p_x, p_y, and p_z contribution in DOS. (For interpretation of the references to color in this legend, the reader is referred to the web version of the article.)

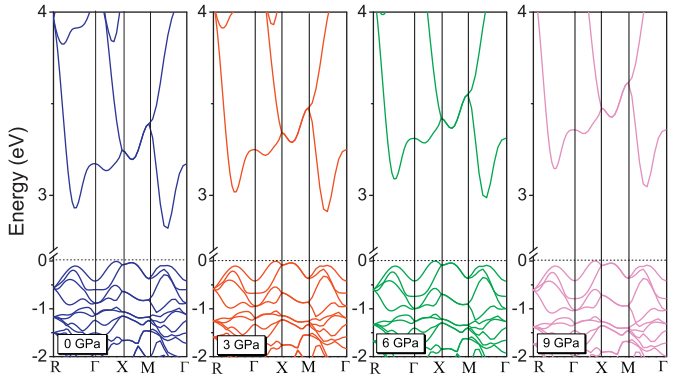

Fig. 5. The band structure of an α-TeO_2 crystal under different pressures.

5. Optical properties

By studying optical properties of materials, it can be possible to propose new potential optoelectronic applications. The calculation of complex dielectric function can be considered as one of the best approaches to investigate the optical properties of materials. The complex dielectric function is a tool to identify all optical aspects such as reflectivity percentage as well as absorption spectrum. The complex dielectric function is made up of two contributions; real part and imaginary part, which are related to the following equation:

$$\varepsilon_{complex} = \Re\varepsilon + i\Im\varepsilon, \tag{3}$$

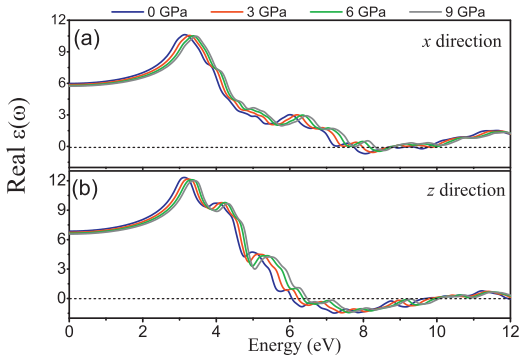

Fig. 6. The real part of the complex dielectric function of an α-TeO_2 crystal under hydrostatic pressure up to 9 GPa. (For interpretation of the references to color in the text, the reader is referred to the web version of the article.)

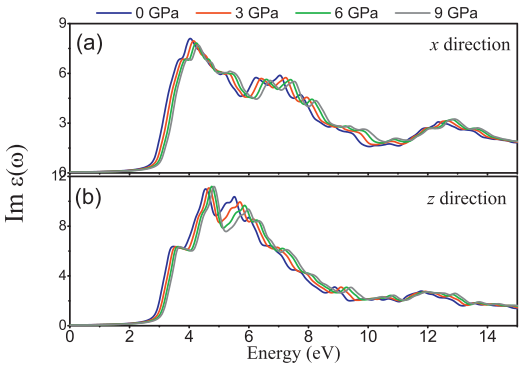

Fig. 7. The imaginary part of the complex dielectric function of an α-TeO_2 crystal under hydrostatic pressure up to 9 GPa.

The imaginary component of the dielectric function is identified through Eq. (3), which takes interband optical transitions between occupied (ik) and unoccupied electron states (fk) [20] into account,

$$\Im\varepsilon^{\alpha\alpha}(\omega) = \frac{4\pi e^2}{m^2\omega^2}\sum_{i,f}\int\frac{2d^3k}{(2\pi)^3}|\langle ik|P_\alpha|fk\rangle|^2 f_i^k(1-f_f^k)\delta(E_f^k - E_i^k - \hbar\omega), \tag{4}$$

the real part of the dielectric function is obtained correspondingly:

$$\Re\varepsilon^{\alpha\beta}(\omega) = \delta_{\alpha\beta} + \frac{2}{\pi}Pr.\int_0^\infty \frac{\Im\varepsilon^{\alpha\beta}(\omega')}{\omega'^2-\omega^2}\omega' d\omega', \tag{5}$$

where Pr. denotes to the Cauchy principal value.

The real and the imaginary parts of the complex dielectric function of the α-TeO_2 crystal under hydrostatic pressure up to 9 GPa are plotted in Figs. 6 and 7 respectively. As seen in Fig. 6, by increasing the imposed hydrostatic pressure, the real part of the complex dielectric function is slightly shifted to higher energies (blue shift). Also the static dielectric constant decreases by increasing the pressure. Needless to say that the almost unchanging value of the $\Re\varepsilon$ is originated by the semiconductor nature of the considered material.

For more details investigation on the optical properties of the α-TeO_2, two important optical spectra are discussed: the optical absorption and the reflectivity spectrum. The optical absorption and the reflectivity spectrum of the α-TeO_2 crystal under different hydrostatic pressures are plotted in Figs. 8 and 9, respectively.

Considering Fig. 8, one can see that α-TeO_2 crystal indicates almost same optical gap in both polarization directions, which is due to the excitation behaviors of the valance electrons in these two directions. Following Fig. 9, it can be seen from the reflectivity spectra of α-TeO_2 under 0, 3, 6 and 9 GPa there exists a considerable anisotropy between the two components along the x and z polarization directions, as the z-component show higher reflectivity than that of x-component.

Finally, the energy loss spectrum of the α-TeO_2 is plotted in Fig. 10. The peak of the energy loss spectrum indicates the plasma frequency of the compound. According to Fig. 10, the plasma frequency of the α-TeO_2 is observed somewhere between 24 and 25 eV.

The optical properties are calculated in the energy range 0–30 eV, but we show the spectral structure of the optical properties in the energy range where it exhibits the intensive spectral features.

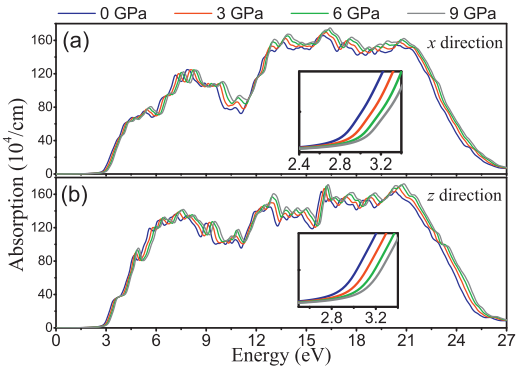

Fig. 8. The optical absorption of an α-TeO_2 crystal under different hydrostatic pressures.

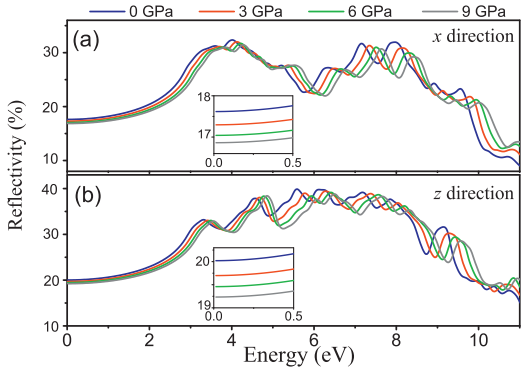

Fig. 9. The reflectivity spectrum of an α-TeO_2 crystal under different hydrostatic pressures.

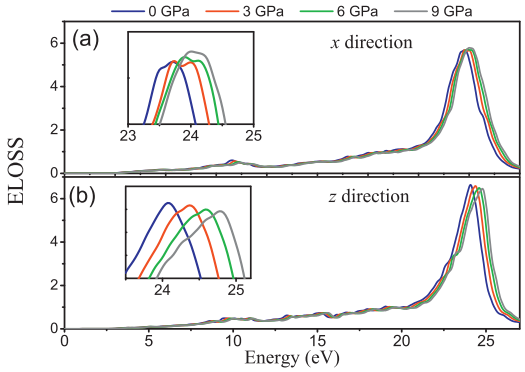

Fig. 10. The energy loss spectrum of an α-TeO_2 crystal under different hydrostatic pressures.

6. Conclusions

Using the optimized structure of α-TeO_2, we have calculated the structural properties of α-TeO_2 under pressure between 09 GPa. The calculated lattice parameters show good agreement with the previous results. It has been found that the α-TeO_2 exhibits two different bond lengths. The calculated electronic charge density distribution confirms the covalence nature for the Te–O bonds. The structural stability of the cell, is confirmed by cohesive energy calculation. The calculated electronic band structure, density of states and the optical properties confirm that the energy band gap increases with rising the pressure. The calculated optical properties give deep insight into the electronic structure.

Acknowledgements

This work is supported by Kermanshah Branch, Islamic Azad University, Kermanshah, Iran. A.H. Reshak would like to acknowledge the CENTEM project, reg. no. CZ.1.05/2.1.00/03.0088, co-funded by the ERDF as part of the Ministry of Education,

Youth and Sports OP RDI program and, in the follow-up sustainability stage, supported through CENTEM PLUS (LO1402) by financial means from the Ministry of Education, Youth and Sports under the National Sustainability Program I. Computational resources were provided by MetaCentrum (LM2010005) and CERIT-SC (CZ.1.05/3.2.00/08.0144) infrastructures. M. Naseri would like to thank Soheila Gholipour, Yasna Naseri and Viana Naseri for their interests in this work.

References

[1] Y. Li, W. Fan, H. Sun, X. Cheng, P. Li, X. Zhao, Structural, electronic, and optical properties of α, β, and γ-TeO_2, J. Appl. Phys. 107 (2010) 093506.
[2] P.A. Thomas, The crystal structure and absolute optical chirality of paratellurite α-TeO_2, J. Phys. C 2 1 (1988) 4611.
[3] D.M. Korn, A.S. Pine, G. Dresselhaus, T.B. Reed, Infrared reflectivity of paratellurite, TeO_2, Phys. Rev. B 8 (1973) 768.
[4] V.H. Beyer, Z. Kristallogr. 124 (1967) 124–228.
[5] S. Blanchandin, P. Marchet, P. Thomas, J.C. Champarnaud-Mesjard, B. Frit, Equilibrium and non-equilibrium phase diagram within the TeO_2-rich part of the TeO_2–Nb_2O_5 system, J. Mater. Chem. 9 (1999) 1785–1788.
[6] J.C. Champarnaud-Mesjard, S. Blanchandin, P. Thomas, A.P. Mirgorodsky, T. Merle-Mejean, B. Frit, Crystal structure, Raman spectrum and lattice dynamics of a new metastable form of tellurium dioxide: γ-TeO_2, J. Phys. Chem. Solids 61 (2000) 1499–1507.
[7] N. Dewan, K. Sreenivas, V. Gupta, Comparative study on TeO_2 and TeO_3 thin film for γ-ray sensor application, Sens. Actuators A 147 (2008) 115–120.
[8] M. Ceriotti, F. Pietrucci, M. Bernasconi, Ab initio study of the vibrational properties of crystalline TeO_2: the α, β, and γ phases, Phys. Rev. B 73 (2006) 104304.
[9] V.L. Deringer, R.P. Stoffel, R. Dronskowski, Thermochemical ranking and dynamic stability of TeO_2 polymorphs from ab initio theory, Cryst. Growth Des. 14 (2014) 871–878.
[10] Y. Ohmachi, N. Uchida, Temperature dependence of elastic, dielectric, and piezoelectric constants in TeO_2 single crystals, J. Appl. Phys. 41 (1970) 2307.
[11] P.A. Thomas, The crystal structure and absolute optical chirality of paratellurite, α-TeO_2, J. Phys. C 21 (1988) 4611.
[12] J.C. Champarnaud-Mesjard, S. Blanchndin, P. Thomas, A.P. Mirgorod-sky, T. Merle-Mejean, B. Frit, Crystal structure, Raman spectrum and lattice dynamics of a new metastable form of tellurium dioxide: γ-TeO_2, J. Phys. Chem. Solids 61 (2000) 1499–1507.
[13] Y. Ohmachi, N. Uchida, The crystal structure and absolute optical chirality of paratellurite, α-TeO_2, J. Appl. Phys. 41 (1970) 2307.
[14] X. Liu, al. et, Phase transition and equation of state of paratellurite (TeO_2) under high pressure, Mater. Res. Express 3 (2016) 076206.
[15] P. Blaha, K. Schwarz, G.K.H. Madsen, D. Kvasnicka, J. Luitz, K. Schwarz, An Augmented Plane Wave, 2001, ISBN 3-9501031-1-2.
[16] J.P. Perdew, K. Burke, M. Ernzerhof, Generalized gradient approximation made simple, Phys. Rev. Lett. 77 (1996) 3865–3868.
[17] H.J. Monkhorst, J.D. Pack, Special points for Brillouin-zone integrations, Phys. Rev. B 13 (1995) 5188.
[18] H. Ehrenreich, M.H. Cohen, Self-consistent field approach to the many-electron problem, Phys. Rev. 115 (1959) 786–790.
[19] F. Birch, Equation of state and thermodynamic parameters of NaCl to 300 kbar in the high-temperature domain, J. Geophys. Res. B 83 (1978) 1257–1268.
[20] R. Abt, C. Ambrosch-Draxl, P. Knoll, Optical response of high temperature superconductors by full potential LAPW band structure calculations, Phys. B: Condens. Matter 194196 (1994) 1451–1452.
[21] P.A. Thomas, The crystal structure and absolute optical chirality of paratellurite, α-TeO_2, J. Phys. C 21 (1988) 4611.
[22] N. Berkaine, E. Orhan, O. Masson, P. Thomas, J. Junquera, Nonlinear optical properties of TeO_2 crystalline phases from first principles, Phys. Rev. B 83 (2011) 245205.
[23] M. Ceriotti, F. Pietrucci, M. Bernasconi, Ab initio study of the vibrational properties of crystalline TeO_2: the α, β, and γ phases, Phys. Rev. B 73 (2006) 104304.
[24] M.B. Yahia, E. Orhan, A. Beltran, O. Masson, T. Merle-Mejean, A. Mirgorodski, P. Thomas, Theoretical third-order hyperpolarizability of paratellurite from the finite field perturbation method, J. Phys. Chem. B 112 (2008) 10777.